concentration. It is also reported that the viscosity reaches its maximum value at $x = 0.22$.[31] The cluster distribution does not change so much in region c ($0.18 \leq x \leq 0.5$) for both the increases of alcohol concentration and liquid temperature (Figure 4C and 4D). In regions c and d, the water-to-ethanol molar ratio is smaller than 5. This number means that any ethanol molecule is almost always in contact with at least one ethanol molecule stochastically. Under this condition, the following association-dissociation equilibrium should be considered as an important process among various association equilibria in the solution.

$$(C_2H_5OH)_{m-1} + C_2H_5OH \overset{K_{m,0}}{\rightleftharpoons} (C_2H_5OH)_m \quad (5)$$

This type of equilibria was first considered by Kempter and Mecke[32] and modified for the elucidation of the infrared absorption of various alcoholic solutions by Coggeshall and Saier.[33]

As seen from the temperature independence of the spectral patterns, the enthalpy change of this process is much smaller than 1 kcal/mol in region c ($0.18 \leq x \leq 0.5$). This means that the equilibrium constant $K_{m-1}{}^{n+1}$ of the following exchange process is close to unity in the cluster region observed ($4 < m < 9$).

$$(C_2H_5OH)_m + (C_2H_5OH)_n \overset{K_{m-1}{}^{n+1}}{\rightleftharpoons} (C_2H_5OH)_{m-1} + (C_2H_5OH)_{n+1} \quad (6)$$

Namely, $[(C_2H_5OH)_{m-1}]/[(C_2H_5OH)_m] \approx [(C_2H_5OH)_n]/[(C_2H_5OH)_{n+1}] \approx$ constant. Figure 3 shows that this relation holds approximately for the parent cluster sizes larger than 4 in the solutions with ethanol concentrations of 40-80% ($0.17 \leq x \leq 0.56$). The association equilibrium (reaction 6) with $K_{m-1}{}^{n+1} \approx 1$ is characteristic of the solutions in region c.

In ethanol rich solutions with $x > 0.5$, larger ethanol polymers tend to dissociate with increasing ethanol content and temperature. Long linear chains must be unstable in the solutions with insufficient water molecules where the direct interaction between the ethyl groups (forming hydrophobic bonds) may induce three-dimensional structural change of ethanol clusters.

VI. Conclusion

The isolation of hydrogen-bonding clusters from ethanol-water solutions through adiabatic expansion of mist particles under vacuum revealed the following characteristics of the ethanol-water and ethanol-ethanol clustering in the solutions: (1) The hydrophobic hydration of ethanol is so strong that pure water clusters are not detectable at $x > 0.04$. (2) Ethanol molceules tend to form ethanol polymer chains with surrounding water molecules which make up hydration shells around ethyl groups at the region of $x < 0.04$, but at $x > 0.08$ the hydrogen bonding between water molecules becomes very weak compared with the ethanol-ethanol bond.

Registry No. CH_3OH, 67-56-1.

(31) *International Critical Tables, National Research Council*; McGraw-Hill: New York and London, 1929; p 22.
(32) Kempter, H.; Mecke, R. *Z. Phys. Chem.* **1941**, *16*, 220.
(33) Coggeshall, N. D.; Saier, E. L. *J. Am. Chem. Soc.* **1951**, *73*, 5414.

Carbonaceous Solids as a Model for Adsorption by Dispersion Forces

Edward M. Arnett,* Brenda J. Hutchinson, and Marguerite H. Healy

Contribution from the Department of Chemistry, Duke University, Durham, North Carolina 27706. *Received November 6, 1987*

Abstract: Heats of adsorption of many liquids of widely varying structure are reported on several carbonaceous solids: graphite, anthracite coal, Ambersorb XE-348, and two graphitized carbon blacks, Carbopack B and F. Heats of adsorption on the two graphitized carbon black samples correlate closely with the polarizabilities of the adsorbate and the number of main group atoms in the molecules as might be expected for dispersion force interactions; there is no relationship to the basicities of the adsorbates. Except for the two graphitized carbon black samples, Carbopack B and F, correlation between the various types of carbonaceous solids is poor.

Acid-base chemistry has been used successfully as a means for reducing the complexities of chemical behavior for millions of compounds to a manageable number of parameters. All organic compounds are acids, bases, or both, and most of them can be activated through interactions with other acids or bases. In recent years classical acid-base scales in water at 25 °C[1-3] have been extended to a variety of other solvents and, most significantly, to the gas phase.[4-10] By comparing acid-base properties in these different media there has been considerable success in separating acid-base properties that are inherent to the molecular structures of the isolated acid and base molecules from those properties that are induced by interaction with surrounding solvent.

Many, if not most, reactions of biological and industrial importance occur at liquid-liquid interfaces (micelles, vesicles, etc.)

(1) Bell, R. P. *The Proton in Chemistry*, 2nd ed.; Cornell University Press: Ithaca, 1973.
(2) Kortum, G.; Vogel, W.; Andrusson, K. *Dissociation Constants of Organic Acids in Aqueous Solution*; Butterworths: London, 1961.
(3) (a) Perrin, D. D. *Dissociation Constants of Organic Bases in Aqueous Solution*; Butterworths: London, 1965. (b) Perrin, D. D. *Dissociation Constants of Organic Bases in Aqueous Solution, Supplement*; Pergamon Press: New York, 1982.
(4) Davis, M. M. In *The Chemistry of Non-Aqueous Solvents*; Lagowski, J. J., Ed.; Academic: New York, 1970; Vol. 3.
(5) Arnett, E. M.; Scorrano, G. *Adv. Phys. Org. Chem.* **1976**, *13*, 84.
(6) (a) Taft, R. W. *Prog. Phys. Org. Chem.* **1982**, *14*, 1. (b) Taft, R. W. *Kinetics of Ion-Molecule Reactions*; Ausloos, P., Ed.; New York, 1979. (c) Taft, R. W. *Proton Transfer Reactions*; Caldin, E., Gold, V., Eds.; Chapman and Hall: London, 1975.
(7) Bower, M. T. *Gas Phase Ion Chemistry*; Academic Press: New York, 1979; Vol. 2.
(8) "Evaluated Gas Phase Basicities and Proton Affinities of Molecules; Heats of Formation of Protonated Molecules": Lias, S. G.; Liebman, J. F.; Levin, R. D. *J. Phys. Chem. Ref. Data* **1984**.
(9) Arnett, E. M. *Acc. Chem. Res.* **1973**, *6*, 404.
(10) Arnett, E. M. *J. Chem. Educ.* **1985**, *62*, 385.

0002-7863/88/1510-5255$01.50/0

or at the surfaces of solids rather than in homogeneous media. The study of the adsorption of gases and liquids on solid surfaces is similar in principle to that of solution chemistry in homogeneous systems. Yet, traditionally, the study of adsorption on heterogeneous systems has been treated as a separate area of physical chemistry with a special focus on catalysis, because of its industrial importance.

The present article extends our efforts to increase the understanding of heterogeneous acid–base chemistry by applying the principles that have been successful for analyzing homogeneous systems. The goal of our approach is to model heterogeneous systems by homogeneous analogues. Previously we have demonstrated that the acid–base behavior of a microreticular sulfonic acid resin is modeled well by solutions of *p*-toluenesulfonic acid.[11] Similarly, heats of interaction of silica with a series of basic liquids confirmed the inference that this solid interacts primarily by virtue of its hydrogen-bonding sites in a manner that is modeled much better by homogeneous solutions of phenols than by protonic acids.[12] As of this writing, we have been unable to identify a solid whose properties are modeled exclusively by Lewis acids (e.g., $SbCl_5$, BF_3). An attempt to apply our thermochemical method of solid acid classification has been combined with an FT–IR study of several aluminas with generally ambiguous results.[13] The overall goal of our research is to model the adsorption properties of complex solids, such as coals, by multiparameter equations containing contributions from proton transfer, hydrogen-bonding, Lewis acidity, and dispersion forces.[14] The focus of this paper is to gain an understanding of the effects of dispersive interactions in adsorption on solid systems. These dispersive interactions are present in all adsorption processes, and an understanding of them is necessary to be able to isolate acid–base interactions from measured adsorption properties.

The importance of dispersive interactions in homogeneous systems has been demonstrated by Taft and Kamlet. They[15-17] have had great success correlating an enormous number of chemical processes in condensed phases using a multiparameter equation which includes contributions from molar volume ($\bar{V}$), dipolarity (π^*), polarizability (∂), hydrogen-bonding acidity (α), and hydrogen-bonding basicity (β). They found, however, that a term which corresponds to a dispersion interaction, log L^{16}, was necessary when transferring a solute from the gas phase to solution.[18] The term L^{16} refers to the Ostwald solubility coefficient in *n*-hexadecane at 25 °C as determined by Abraham et al.[19]

Interactions of acids and bases are usually exothermic processes (15–50 kcal/mol) and take place at highly specific functionality sites. Adsorption processes are classified traditionally as either "chemical" or "physical" depending on the nature of the forces involved. In "chemical" adsorption an atom or molecule is bound to the surface by the formation of some type of localized chemical bond. In contrast, "physical" adsorption occurs as a result of relatively nonspecific intermolecular forces classified as van der Waals, London, and dispersion forces. These nonspecific intermolecular forces are the result of the motion of electrons in molecules, so that at any instant the average centers of positive and negative charge do not coincide. The electric field surrounding a molecule induces dipole moments in other nearby molecules, leading to attraction. Depending on the number of bonds and electrons in each molecule such forces are cumulative, being more or less proportional to the sizes of the molecules. Dispersion interactions play the determining role in adsorption of almost all gases and vapors on carbonaceous adsorbents.[20] Accordingly, we have looked for an appropriate solid adsorbent that could serve as a prototype for dispersion forces in the same way that we have used sulfonic acid resins[11] and silica[12] as prototypes for proton transfer and hydrogen-bonding, respectively. As possible solid models for nonspecific adsorbents we have chosen several types of carbonaceous materials: graphite, anthracite coal, Ambersorb XE-348, Carbopack B, and Carbopack F.

Carbon occurs in its elemental form as crystalline or amorphous solids. Graphite and diamond are crystalline forms while carbon black is an example of an amorphous form. The ideal structure of graphite[21,22] is described as plane layers of carbon atoms that are bonded covalently in a regular open-centered hexagonal array stacked in ABAB sequence with weak van der Waals bonding between the layers. The "free valences" which exist at the edges of the graphitic layer planes of microcrystalline carbon, however, are very reactive and form compounds with any suitable foreign atom present.[22] Anthracite coal, a coal of high carbon content, may be considered as predominately an amorphous form of carbon. It has a fixed carbon content of 92–98%.[23] Ambersorb XE-348 is produced by the pyrolysis of a sulfonated macroreticular styrene–divinylbenzene copolymer. When the copolymer is heated

Table I. Heats of Adsorption by Gas–Solid Chromatography of Various Compounds on Graphite, Anthracite Coal, and Carbopack F

solute	$-\Delta H$ (graphite) (kcal/mol)	$-\Delta H$ (anthracite) (kcal/mol)	$-\Delta H$ (Carbopack F) (kcal/mol)
ethylenediamine	8.43 ± 0.25	11.62 ± 0.21	
2-methylpyridine	8.70 ± 0.23	9.81 ± 0.24	10.70 ± 0.17
benzene	9.43 ± 0.70		8.99 ± 0.09
acetonitrile	9.63 ± 0.70		
3-methylpyridine	9.87 ± 0.45	9.54 ± 0.25	11.15 ± 0.22
pyridine	10.03 ± 0.12	9.49 ± 0.41	8.92 ± 0.08
triethylamine	10.18 ± 0.20		9.16 ± 0.15
cyclohexylamine	10.40 ± 0.30	11.90 ± 0.43	9.69 ± 0.09
toluene	10.47 ± 0.43	10.47 ± 0.10	10.49 ± 0.28
cyclohexanone	10.92 ± 0.31	13.51 ± 0.51	9.65 ± 0.19
pyrrolidine	11.10 ± 0.23	14.95 ± 0.52	
hexane	11.19 ± 0.15		9.55 ± 0.11
2,6-dimethylpyridine	11.26 ± 0.25	9.71 ± 0.19	12.02 ± 0.10
bromobenzene	11.37 ± 0.39	11.49 ± 0.15	11.68 ± 0.37
anisole	11.66 ± 0.13	10.23 ± 0.12	12.17 ± 0.11
n-butylamine	12.19 ± 0.68		8.56 ± 0.15
2,4,6-trimethylpyridine	12.45 ± 0.50	9.90 ± 0.17	13.51 ± 0.32
propylene carbonate	12.68 ± 0.59		9.96 ± 0.48
dimethyl sulfoxide	12.86 ± 0.69	13.22 ± 0.30	9.69 ± 0.28
benzonitrile	14.14 ± 0.47	10.58 ± 0.42	11.75 ± 0.14
nitrobenzene	14.22 ± 0.43	11.53 ± 0.48	12.74 ± 0.25
2,6-di-*tert*-butylpyridine	15.31 ± 0.67	11.27 ± 0.27	14.62 ± 0.35
octylamine	15.73 ± 0.44	12.26 ± 0.56	13.71 ± 0.28
4-methylpyridine		10.41 ± 0.09	11.29 ± 0.25
dodecane			16.44 ± 0.16
n-butylbenzene			14.30 ± 0.41
octane			11.99 ± 0.19
nonane			13.55 ± 0.34
n-hexylamine			11.62 ± 0.29
undecane			15.04 ± 0.29
1-bromohexane			11.68 ± 0.37
o-bromoanisole			14.54 ± 0.29
p-bromoanisole			14.64 ± 0.37
1-chlorooctane			14.21 ± 0.46

(11) Arnett, E. M.; Haaksma, R. A.; Chawla, B.; Healy, M. H. *J. Am. Chem. Soc.* **1986**, *108*, 4888.
(12) Arnett, E. M.; Cassidy, K. F. *Rev. Chem. Intermed.* **1988**, *9*, 27.
(13) Healy, M. H.; Wiserman, L. F.; Arnett, E. M.; Wefers, K. "Infrared Spectroscopy and Microcalorimetric Investigations of Delta-Theta and Kappa Aluminas using Basic Probe Molecules: Acetonitrile, Pyridine, 2,6-Lutidine, and *n*-Butylamine", submitted for publication.
(14) Arnett, E. M.; Gumkowski, M.; Liu, Q. *Energy and Fuels* **1988**, *2*, 295.
(15) Kamlet, M. J.; Doherty, R. M.; Abraham, M. H.; Carr, P. W.; Doherty, R. F.; Taft, R. W. *J. Phys. Chem.* **1987**, *91*, 1996.
(16) Taft, R. W.; Abboud, J.-L. M.; Kamlet, M. J.; Abraham, M. H. *J. Solution Chem.* **1985**, *14*(*3*), 153.
(17) Kamlet, M. J.; Abboud, J. L.; Taft, R. W. *J. Am. Chem. Soc.* **1977**, *99*(*18*), 6027.
(18) Abraham, M. H.; Grellier, P. L.; McGill, R. A.; Doherty, R. M.; Kamlet, M.; Hall, T. M.; Taft, R. W.; Carr, P. W.; Koros, W. J. *Polymers* **1987**, *28*, 1363. An extensive search of the literature has failed to produce another data set which overlaps as extensively with our results or which correlates as well with them; see, however: Fuchs, R.; Stephenson, K. W. *Can. J. Chem.* **1985**, *63*, 349.
(19) Abraham, M. H.; Grellier, P. L.; McGill, R. A. *J. Chem. Soc., Perkin Trans. II* **1987**, *6*, 797.
(20) Dubnin, M. M. *Carbon* **1980**, *18*, 355.
(21) Fischback, D. B. In *Chemistry and Physics of Carbon*; Walker, P. L., Jr., Ed.; Marcel Dekker, Inc: New York, 1971; Vol. 7.
(22) *Kirk-Othmer Encyclopedia of Chemical Technology*, 3rd ed.; John Wiley and Sons, Inc.: New York, 1978; Vol. 4.
(23) Speight, J. G. *The Chemistry and Technology of Coal*; Marcel Dekker, Inc.: New York, 1983.

Table II. Heats of Adsorption of Various Compounds on Ambersorb XE-348 and Carbopack B by Flow Calorimetry (Microscal)

solute	$-\Delta H$(Ambersorb) (mcal/g)	$-\Delta H$(Carbopack B) (mcal/g)
cyclohexanone	79.2 ± 3.1	
hexane	388.2 ± 30.1	44.0 ± 0.7
tert-butylamine	339.7 ± 29.8	5.9 ± 0.2
pyridine	607.2 ± 9.1	24.7 ± 1.0
triethylamine	619.0 ± 18.7	20.5 ± 2.6
isopropylamine	886.4 ± 27.2	
3-methylpyridine	925.1 ± 34.5	
2-methylpyridine	937.2 ± 20.2	
4-methylpyridine	968.4 ± 46.2	
toluene	981.4 ± 11.0	41.0 ± 1.4
2,4,6-trimethylpyridine	984.6 ± 35.4	199.7 ± 8.9
2,6-dimethylpyridine	1221.7 ± 49.8	117.5 ± 5.1
n-butylamine	1387.0 ± 115.9	27.5 ± 4.2
ethylenediamine	1640.1 ± 7.7	
pyrrolidine	2588.0 ± 165.8	
benzene		18.0 ± 1.5
2,6-di-*tert*-butylpyridine		93.2 ± 4.5
benzonitrile		103.0 ± 3.2
octylamine		249.8 ± 11.9

in an inert atmosphere, a series of chemical reactions occur which transform the porous starting material into a carbon replica of the original polymer.[24] The manufacturer, Rohm and Haas, states that Ambersorb XE-348 has properties similar to those of activated carbon. Carbopack B and F are graphitized carbon blacks.[25] The heat treatment of a carbon black sample under vacuum in an inert gas atmosphere to 3000 °C yields polyhedral particles with all of the faces the same: the basal plane of graphite.[26,27] The homogeneity of the external surface of the particles makes graphitized carbon black an ideal surface for theoretical studies.

As before[12] we have used the heat of adsorption determined either by gas–solid chromatography or flow calorimetry as the experimental method for quantifying adsorbate–adsorbent interactions. The results are then compared with each other and with appropriate physical parameters (e.g., polarizability, log L[16], number of main group atoms) that are usually considered to represent interactions through dispersion forces.

Experimental Section

Thermodynamic results are presented here for a series of carbonaceous adsorbents: graphite, anthracite coal, Ambersorb XE-348, Carbopack B, and Carbopack F. The heats of adsorption of a series of bases on graphite, anthracite coal, and Carbopack F were determined with use of gas–solid chromatography (GSC) (Table I). The Microscal flow calorimeter was used to determine the heats of adsorption of a series of bases on Ambersorb XE-348 and Carbopack B (Table II). The surface areas of graphite, anthracite coal, Ambersorb XE-348, Carbopack B, and Carbopack F were determined by BET analysis.

A. General Procedures. 1. Solvents. All glassware was dried in an oven at 125 °C for 12 h and cooled in a desiccator prior to use. All compounds used in these studies were available commercially and were purified by standard techniques.[28] Each liquid was refluxed for at least 1 h with the appropriate drying agent before collection of the middle fraction. The purity of the compounds was checked by comparison of their boiling points to published values.[28,29] Following purification, all compounds were stored in a desiccator and were used within 14 days to minimize decomposition and water contamination. All distillations and other manipulations at atmospheric pressure were done under argon. Water content was checked periodically with a Mettler DL18 Karl Fischer Apparatus and was found to be less than 500 ppm before experiments.

For flow calorimetry studies, acetonitrile was chosen as the carrier solvent to ensure that the adsorption of the solute from the solution was the dominant process. For a low- or medium-energy surface (e.g., graphitized carbon black) a polar solvent should be used to minimize solvent effects.[30] Acetonitrile (Mallinckrodt) was stirred with anhydrous potassium carbonate for approximately 24 h and fractionally distilled from phosphorous pentoxide through a Vigreux column under argon. The middle fraction was collected directly in a solvent bottle equipped with an automatic zeroing solvent buret. The solvent was stored under a positive pressure of argon and was used for experiments only if its water content, as measured by Karl Fischer, was below 100 ppm.

2. Solids. The graphitized carbon black samples manufactured by Supelco, Carbopack B, lot number A368, 60/80 mesh, and Carbopack F, special order, 60/80 mesh, were activated by heating at 150 °C in a vacuum oven evacuated to a final pressure of <2.0 cmHg for approximately 12 h. At the completion of this procedure the oven was filled with air, predried by passage through a drying tube of phosphorous pentoxide. The samples were then transferred to a Kewaunee Model No. 4091 drybox. The drybox was maintained at a relative humidity of 1 to 2% by constantly pumped circulation of nitrogen through a trap cooled to −72 °C by a Neslab Cryocool CC-60 system.

Ambersorb XE-348, lot No. 0015, a carbonaceous macroreticular adsorbent supplied by Rohm and Haas, was activated at 50 °C and a final pressure of <1 cmHg for approximately 48 h. The samples were transferred and stored in the drybox.

B. Techniques. 1. Gas–Solid Chromatography (GSC). The gas–solid chromatographic studies of graphite and anthracite coal were conducted with a Hewlett Packard 5700A gas chromatograph equipped with a thermal conductivity detection system. GSC studies of Carbopack F were conducted with a Hewlett Packard 5890A gas chromatograph with a flame ionization detector.

Two, 3.0 m, 1.5 mm internal diameter, metal columns were packed with graphite (Alfa Products, lot 040980, 60/80 mesh) and activated under a helium flow at 300 °C for 24 h. The carrier gas, helium (National Welders), was passed through a Supelco gas purifier prior to use. The flow rate for the GSC study of graphite was 27.3 mL/min.

Two, 2.0 m, 1.5 mm internal diameter, metal columns were packed with anthracite coal, 25/60 mesh, sample No. PSOC-1461 from the Coal Research Section of the Pennsylvania State University, and activated under a helium flow at 300 °C for 48 h. The flow rate for the GSC study of anthracite coal was 50.0 mL/min.

A 3 ft, 2 mm internal diameter, glass column was packed with 60/80 mesh Carbopack F and activated under a flow of nitrogen at 300 °C for 24 h. The flow rate for the GSC study of Carbopack F was 24.0 mL/min.

The GSC studies of graphite and Carbopack F were carried out in the "infinite-dilution" range. A sample of each base in anhydrous diethyl ether was injected onto the column at a series of temperatures. The equilibrium partition coefficient, K_r, at each temperature was calculated from the retention time of the base[31]

$$K_r = V_n/(A_s w_s) = [(j)(F_c)(t_r - t_a)]/(A_s w_s) \quad (1)$$

where V_n is the net retention volume, A_s is the specific surface area of the solid as determined by BET analysis, w_s is the weight of the solid in the column, j is the correction for the pressure drop across the column, F_c is the corrected flow rate, t_a is the retention time of a nonsorbed solute, and t_r is the retention time of the solute.

For the anthracite coal GSC study a neat sample of the base was injected at a series of temperatures. The equilibrium partition coefficient was again calculated from the retention time.

As long as symmetrical peaks are obtained and the retention time is not a function of the sample size the van't Hoff relationship[2] for the temperature dependence of the equilibrium partition coefficient can be

$$\ln K_r = -\Delta H/(RT) + c \quad (2)$$

used to determine the heat of adsorption. The measurements were carried out in the linear portion of the adsorption isotherm, where lateral interactions are negligible and the heat of adsorption depends exclusively on adsorbate–adsorbent interactions.[32] The heats of adsorption determined with GSC are presented in Table I.

2. Microscal Flow Calorimeter. The Microscal flow calorimeter was designed for the detection of solute–solid interactions and is capable of measuring very small heats of adsorption.[33] The heats of adsorption of

(24) Neely, J. W. *Carbon* **1981**, *19*, 27.
(25) Bruner, F.; Furlani, G.; Magani, F. *J. Chromatogr.* **1984**, *302*, 167.
(26) Graham, D.; Kay, W. S. *J. Colloid Interface Sci.* **1961**, *16*, 182.
(27) Valenzuela, D.; Myers, A. L. *Separation and Purification Methods* **1984**, *13(2)*, 153.
(28) Perrin, D. D.; Armarego, W. L. F.; Perrin, D. R. *Purification of Laboratory Chemicals*, 2nd ed.; Pergamon Press: Oxford, 1980.
(29) *CRC Handbook of Chemistry and Physics*, 61 ed.; Weast, R. C., Ed.; CRC Press: Boca Raton, 1981.
(30) Zettlemoyer, A. C.; Narayan, K. S. In *Chemistry and Physics of Carbon*; Walker, P. L., Jr., Ed.; Marcel Dekker, Inc.: New York, 1966; Vol. 2.
(31) Laub, R. J.; Pesck, K. L. *Physicochemical Applications of Gas Chromatography*; John Wiley and Sons: New York, 1978.
(32) Crescentini, G.; Magani, F.; Mastrogiacomo, A. R.; Palma, P. *J. Chromatogr.* **1987**, *392*, 83.
(33) Groscek, A. J. In *Adsorption at the Gas-Solid and Liquid-Solid Interface*; Rouquerol, J., Sing, K. S. W., Eds.; Elsevier Scientific: Amsterdam, 1982.

a series of bases on Ambersorb XE-348 and Carbopack B were determined with the Microscal flow calorimeter in the equilibrium mode. This has been described previously.[12]

The carrier solvent for all of the flow calorimeter experiments was acetonitrile, and all the studies were done at ambient temperature 22–24 °C. The reaction cell was packed with the solid adsorbent, and the carrier solvent was pumped through the cell for 1 h. Following the equilibration period the recorder was started and a level baseline was determined. The second syringe pump, which contained a solution of known concentration of the base in the carrier solvent, was started. Once the line was free of air, the flow percolating through the calorimeter was changed from pure carrier solvent to a solution of the base in the carrier solvent by means of appropriate switching valves. The heat of interaction produced a displacement of the strip chart recorder. As the flow continued the solid became saturated with the adsorbate, resulting in a return to thermal equilibrium and a subsequent return of the recorder to the baseline.

The heats of adsorption of a series of bases with Ambersorb XE-348 and Carbopack B were determined at a single concentration of adsorbate in acetonitrile, 0.060 ± 0.005 and 0.100 ± 0.005 M, respectively.

Heats of adsorption determined by flow calorimetry are given in Table II. Since we have no means for determining how many moles of solute were adsorbed on the solid, results are given in terms of mcal/g in contrast to the GSC values. To determine the heats of adsorption from these experiments it was necessary to calibrate the Microscal chemically with use of a Setaram C-80 flow calorimeter. There is no accepted standard for calibration of flow calorimeters.

3. Surface Area Measurements. As a means of characterizing the solids used in this study the surface areas of graphite, anthracite coal, Ambersorb XE-348, Carbopack B, and Carbopack F were determined by using a Quantasorb surface area analyzer equipped with a Quantasorb flow controller. Details for the treatment of each solid and specific surface areas are as follows:

Graphite was degassed at 120 °C under a nitrogen flow for 2 h prior to analysis and gave a surface area of 0.440 m^2/g.

Anthracite coal, 25/60 mesh, was degassed at 120 °C for 2 h under a nitrogen flow prior to analysis, and a surface area of 1.35 m^2/g was determined.

Ambersorb XE-348 was degassed under a flow of nitrogen for 2 h at 150 °C. According to the supplier, Rohm and Haas, Ambersorb XE-348 has a surface area of 500 m^2/g. The surface area determined in this laboratory was 528.5 m^2/g.

Carbopack B was degassed for 2 h at 150 °C under a nitrogen flow. The surface area reported by Supelco was 100 m^2/g. The determined surface area was 91.6 m^2/g.

Carbopack F was degassed at 150 °C for 2 h under a flow of nitrogen. Supelco reported that this graphitized carbon black had a surface area of 6 m^2/g. The value determined, 5.93 m^2/g, was well within experimental error. The adsorption–desorption isotherm of Carbopack F showed no hysteresis.

Discussion

Two important facts are immediately obvious from Table III. First, there is absolutely no relationship between the basicities of the adsorbates, as represented by their heats of interaction with Dowex, and their heats of adsorption on Carbopack F. *n*-Butylamine, a classically strong nitrogen base, is the most weakly adsorbed compound while dodecane, a saturated hydrocarbon, is the most strongly adsorbed. As was shown previously,[11] ΔH_{Dowex} is directly proportional to heats of ionization of the bases by *p*-toluenesulfonic acid and to their pK_{BH^+}'s in water.

Second, heats of adsorption on Carbopack F appear to be well correlated with the electronic polarizabilities of the adsorbates. Moreover, among the homologous series in Table III (e.g., the aliphatic amines, substituted pyridines, and straight chain hydrocarbons) *it is the number of main group atoms present rather than their type* which determines the heat of adsorption (Figure 1). Clearly, this behavior fits that anticipated for dispersion force interactions. These results are compatible with a number of previous studies,[34-36] each one limited to a single homologous series.

Polarizability is defined as the dipole moment induced by an electric field of unit strength. Electronic polarizability is a measure

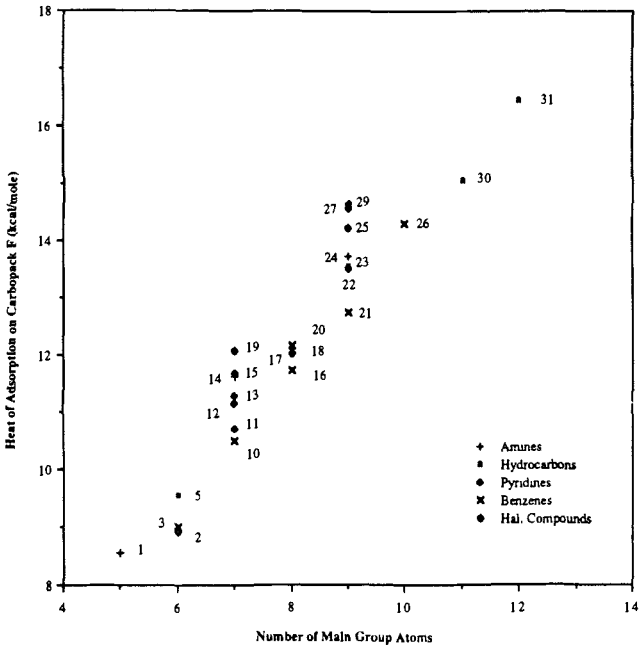

Figure 1. Heats of adsorption by gas–solid chromatography on Carbopack F versus number of main group atoms.

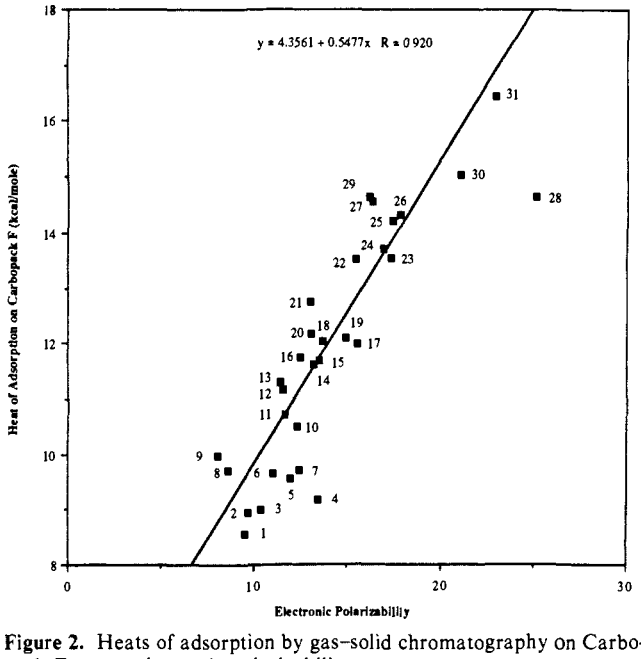

Figure 2. Heats of adsorption by gas–solid chromatography on Carbopack F versus electronic polarizability.

of the ease with which the electrons of a molecule are distorted and is given by

$$\text{electronic polarizability} = [(n^2 - 1)(M)(3)]/[(n^2 + 2)(\rho)(4\pi A)] \quad (3)$$

where n is the refractive index, M is the molecular weight, ρ is the density of the adsorbate, and A is Avogadro's number. Figure 2 portrays the relationship between heats of adsorption on Carbopack F and the electronic polarizability for the compounds in Table III. A slight improvement can be made by recognizing that propylene carbonate, dimethyl sulfoxide, benzonitrile, and nitrobenzene have high dipole moments and that the total polarizability includes a contribution from the orientation polarizability

$$\text{orientation polarizability} = \mu^2/(3kT) \quad (4)$$

where μ is the dipole moment, k is the Boltzman constant, and T is the temperature.

Figure 3 shows a significant improvement over Figure 2, but the point for triethylamine remains significantly removed from

(34) Belyakova, L. D.; Kiselev, A. V.; Kovaleva, N. V. *Anal. Chem.* **1964**, *36*, 1517.
(35) Kiselev, A. V. *Faraday Soc. Discuss.* **1965**, *40*, 205.
(36) Domingo-Garcia, M.; Fernandez-Morales, I.; López-Garzon, F. J.; Moreno-Castillo, C. *J. Chromatogr.* **1984**, *294*, 41.

Table III. Heats of Adsorption by Gas–Solid Chromatography of Various Compounds on Carbopack F, Dowex, and Graphite with Calculated Electronic and Orientation Polarizabilities

solute	$-\Delta H$(Dowex) (kcal/mol)	$-\Delta H$(Carbo F) (kcal/mol)	$-\Delta H$(graphite) (kcal/mol)	electronic polarizability ($m^3 \times 10^{30}$)	orientation polarizability ($m^3 \times 10^{30}$)
1. *n*-butylamine	21.02 ± 1.08	8.56 ± 0.14	12.19 ± 0.68	9.5	14.3
2. pyridine	14.60 ± 0.27	8.92 ± 0.08	10.03 ± 0.12	9.7	35.7
3. benzene		8.99 ± 0.09	9.43 ± 0.70	10.4	0
4. triethylamine	22.85 ± 0.27	9.16 ± 0.15	10.18 ± 0.20	13.4	5.66
5. hexane		9.55 ± 0.11	11.19 ± 0.15	11.9	0
6. cyclohexanone		9.65 ± 0.19		11.0	57.3
7. cyclohexylamine		9.69 ± 0.09	10.40 ± 0.30	12.4	12.2
8. dimethyl sulfoxide		9.69 ± 0.28	12.86 ± 0.69	8.6	173.3
9. propylene carbonate		9.96 ± 0.48	12.68 ± 0.59	8.0	143.8
10. toluene		10.49 ± 0.28	10.47 ± 0.43	12.3	0.74
11. 2-methylpyridine		10.70 ± 0.17	8.70 ± 0.23	11.6	19.3
12. 3-methylpyridine		11.15 ± 0.22	9.87 ± 0.45	11.5	34.5
13. 4-methylpyridine	15.35 ± 0.18	11.29 ± 0.25		11.4	42.5
14. *n*-hexylamine		11.62 ± 0.29		13.2	11.2
15. bromobenzene		11.68 ± 0.37	11.37 ± 0.39	13.5	14.7
16. benzonitrile		11.75 ± 0.14	14.14 ± 0.47	12.5	87.8
17. octane		11.99 ± 0.19		15.5	0
18. 2,6-dimethylpyridine	16.15 ± 0.13	12.02 ± 0.10	11.26 ± 0.25	13.6	16.0
19. 1-bromohexane		12.09 ± 0.22		14.9	28.6
20. anisole		12.17 ± 0.11	11.66 ± 0.13	13.0	9.3
21. nitrobenzene		12.74 ± 0.25	14.22 ± 0.43	13.0	88.4
22. 2,4,6-trimethylpyridine	17.18 ± 0.37	13.51 ± 0.32	12.45 ± 0.50	15.4	20.2
23. nonane		13.55 ± 0.34		17.3	0
24. octylamine	26.41 ± 0.10	13.71 ± 0.28	15.73 ± 0.44	16.9	11.0
25. 1-chlorooctane		14.21 ± 0.46		17.4	22.4
26. *n*-butylbenzene		14.30 ± 0.41		17.8	0
27. *o*-bromoanisole		14.54 ± 0.29		16.3	33.7
28. 2,6-di-*tert*-butylpyridine	13.87 ± 0.58	14.62 ± 0.35	15.31 ± 0.67	25.1	—
29. *p*-bromoanisole		14.64 ± 0.37		16.1	30.1
30. undecane		15.04 ± 0.29		21.0	0
31. dodecane		16.44 ± 0.16		22.9	0

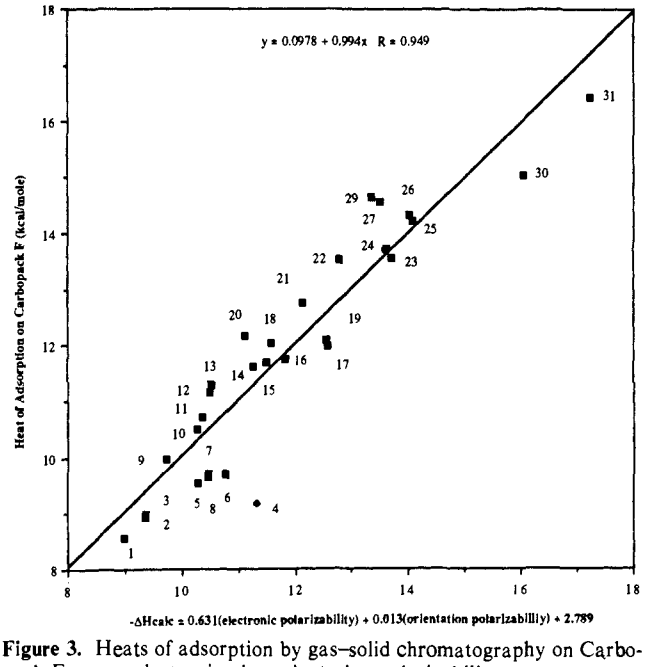

Figure 3. Heats of adsorption by gas–solid chromatography on Carbopack F versus electronic plus orientation polarizability.

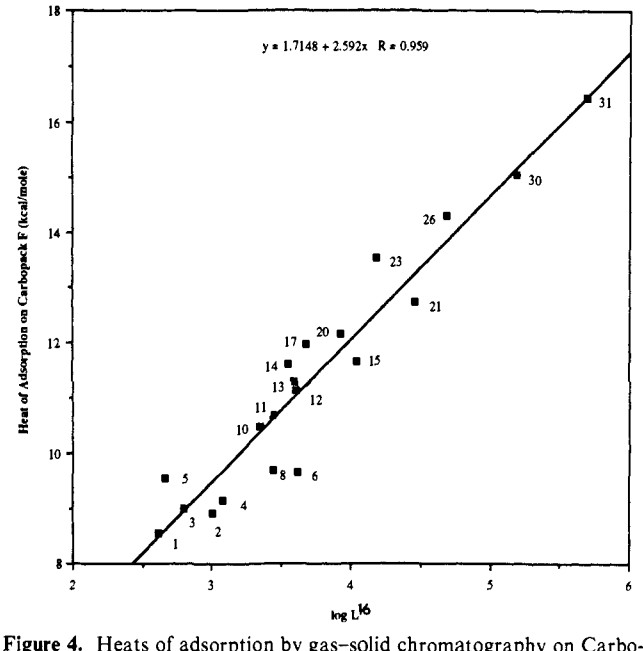

Figure 4. Heats of adsorption by gas–solid chromatography on Carbopack F versus log L^{16}.

the correlation line (the dipole moment for 2,6-di-*tert*-butylpyridine was not available). Unlike all the other molecules in Table III these alone are unable to achieve a conformation where essentially all of the aliphatic or aromatic components of the molecule can lie flat on the carbon surface. This result further implies that the adsorption process on Carbopack F is the result of nonspecific dispersion interactions; for in these interactions the geometry of the adsorbate molecule and of the adsorbent, their mutual orientations, polarizabilities, and the number of electrons are important.[34]

The heats of adsorption on Carbopack F also correlate well with log L^{16} values[18,19] that are indicative of dispersion interactions (Figure 4). This result provides further confirmation that the adsorption process on Carbopack F is the result of nonspecific intermolecular forces.

The ionization potentials of solvent and solute are important contributors to the cohesive part of the free energy of solution.[37] When the heat of adsorption on Carbopack F is correlated with the electronic polarizability plus the ionization potential for 21

(37) Leffler, J. E.; Grunwald, E. *Rates and Equilibria of Organic Reactions*; John Wiley and Sons: New York, 1963.

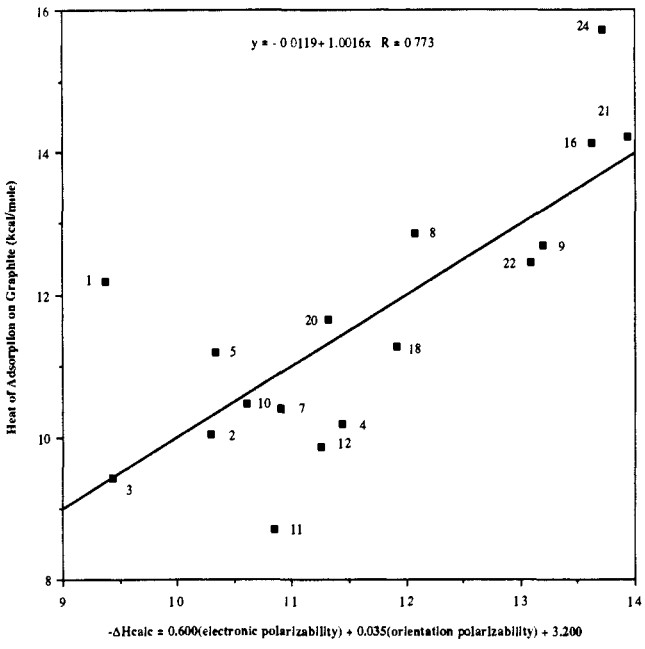

Figure 5. Heats of adsorption by gas–solid chromatography on graphite versus electronic plus orientation polarizability.

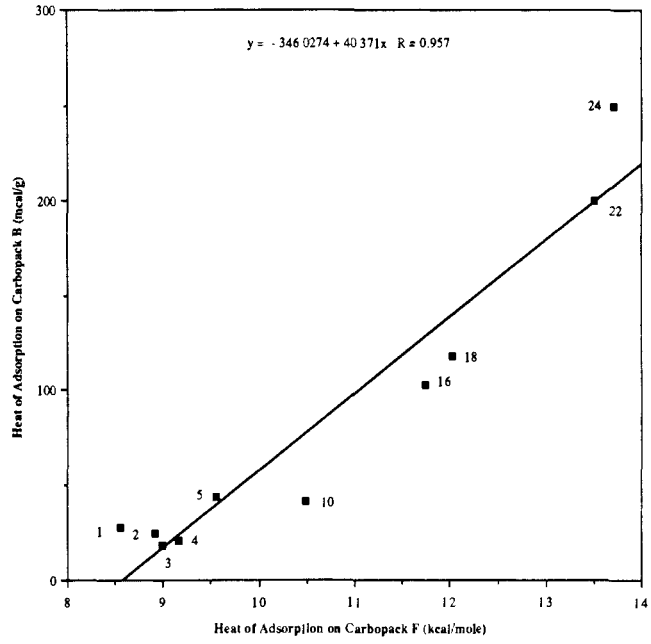

Figure 6. Heats of adsorption by flow calorimetry on Carbopack B versus heats of adsorption by gas–solid chromatography on Carbopack F.

compounds a correlation coefficient of 0.901 results compared to 0.944 for the electronic polarizability plus the orientation polarizability. If all three terms are used a modest improvement to $R = 0.964$ results which is scarcely significant.

Comparison of the Heats of Adsorption on Carbonaceous Solids. The discussion so far has focused on Carbopack F because this solid meets the original criteria for a nonspecific physical adsorbent better than the others tabulated in Tables I and II. Although Carbopack B also meets these criteria the lower surface area of Carbopack F (5.93 m^2/g) relative to Carbopack B (91.6 m^2/g) makes it the adsorbent of choice, since it has been shown that the surface uniformity increases with decreasing surface area.[26]

One interesting result found in the study of graphite is that within a family of compounds (e.g., substituted benzenes, substituted pyridines, aliphatic amines) there are good to excellent correlations between the heats of adsorption and orientation plus electronic polarizability. The overall relationship, however, as shown in Figure 5, is much poorer than that seen with Carbopack F (Figure 3). This is probably the result of small amounts of heterogeneous sites on the surface (e.g., chemical impurities, geometric irregularities) whose influences are masked within families of compounds but are evident when a wide variety of compounds are compared. This trend is not observed with either anthracite coal or Ambersorb XE-348.

Ambersorb XE-348 is a synthetic carbonaceous solid that is marketed as an alternative to granular activated carbon. Selim and El-Nabarawy showed that there was a relationship between the adsorption characteristics of hydrocarbons[38] on activated carbon with their electronic polarizabilities. Similarly, the adsorption characteristics of polar organic compounds[39] on activated carbon are related to their orientation polarizabilities. The calorimetrically determined heats of adsorption with Ambersorb XE-348, however, did not show this behavior. Due to the large particle size and physical strength of the available material it was not possible to perform gas–solid chromatography measurements.

(38) Selim, M. M.; El-Nabarawy, Th. A. *Carbon* **1980**, *18*, 287.
(39) Selim, M. M.; El-Nabarawy, Th. A.; Ghazy, T. M.; Farid, T. *Carbon* **1981**, *19*, 161.

The various types of nonpolar solid systems studied did not correlate with each other. Compared to the generally good correlation between Dowex sulfonic acid resin and a variety of homogeneous systems[11] the present results may seem to be disappointing. These poor correlations are probably the consequence of the variety of types of adsorption sites present on the carbon samples which contribute different combinations of chemical and physical interactions.

Since Carbopack B is also a graphitized carbon black, it is useful to see its relationship to Carbopack F (Figure 6). Clearly the factors that determine adsorption on graphite, anthracite coal, and Ambersorb XE-348 are different from those for the two Carbopacks.

Conclusions

Several types of carbonaceous solids have been compared by heats of adsorption of a variety of polar and nonpolar molecules on their surfaces with gas–solid chromatography and flow calorimetry. Results for two types of graphitized carbon black correlated well with expected behavior based on molecular polarizability and carbon number. More general correlations between these nonpolar solids, however, are not found.

Acknowledgment. This work was supported by the U.S. Department of Energy Grant DE-FG22-85PC80521 and by a grant that was generously provided by the Exxon Educational Foundation.

Registry No. Carbon, 7440-44-0; graphite, 7782-42-5; *n*-butylamine, 109-73-9; pyridine, 110-86-1; benzene, 71-43-2; triethylamine, 121-44-8; hexane, 110-54-3; cyclohexanone, 108-94-1; cyclohexylamine, 108-91-8; dimethyl sulfoxide, 67-68-5; propylene carbonate, 108-32-7; toluene, 108-88-3; 2-methylpyridine, 109-06-8; 3-methylpyridine, 108-99-6; 4-methylpyridine, 108-89-4; *n*-hexylamine, 111-26-2; bromobenzene, 108-86-1; benzonitrile, 100-47-0; octane, 111-65-9; 2,6-dimethylpyridine, 108-48-5; 1-bromohexane, 111-25-1; anisole, 100-66-3; nitrobenzene, 98-95-3; 2,4,6-trimethylpyridine, 108-75-8; nonane, 111-84-2; octylamine, 111-86-4; 1-chlorooctane, 111-85-3; *n*-butylbenzene, 104-51-8; *o*-bromoanisole, 578-57-4; 2,6-di-*tert*-butylpyridine, 585-48-8; *p*-bromoanisole, 104-92-7; undecane, 1120-21-4; dodecane, 112-40-3; pyrrolidine, 616-45-5; acetonitrile, 75-05-8; ethylenediamine, 107-15-3; isopropylamine, 75-31-0.